

MED
T113
+Y12
6983

YALE UNIVERSITY LIBRARY



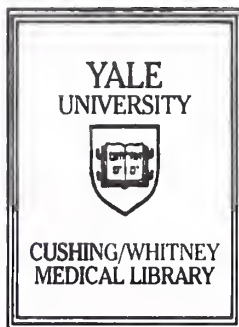
39002010615996

Correlation of Dynamic Contrast Enhanced MRI Imaging
Characteristics with Gene Expression Profiles in
Renal Cell Carcinoma

Essmacel Hussein Abdel-Dayem

YALE UNIVERSITY

2003

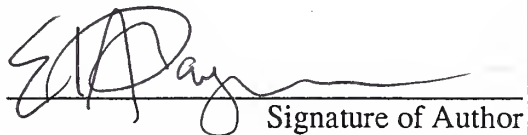


YALE
UNIVERSITY




CUSHING/WHITNEY
MEDICAL LIBRARY

Permission to photocopy or microfilm processing of this thesis for the purpose of individual scholarly consultation or reference is hereby granted by the author. This permission is not to be interpreted as affecting publication of this work or otherwise placing it in the public domain, and the author reserves all rights of ownership guaranteed under common law protection of unpublished manuscripts.


Signature of Author

3/19/03
Date



Digitized by the Internet Archive
in 2017 with funding from
Arcadia Fund

<https://archive.org/details/correlationofdyn00abde>

**Correlation of Dynamic Contrast Enhanced MRI Imaging Characteristics with
Gene Expression Profiles in Renal Cell Carcinoma**

A Thesis Submitted to the
Yale University School of Medicine
in Partial Fulfillment of the Requirements for the
Degree of Doctor of Medicine

by

Essmaeel Hussein Abdel-Dayem

2003

YALE MEDICAL LIBRARY

AUG 14 2003

T 113

T 112

G 983

ABSTRACT:

Correlation of Dynamic Contrast Enhanced MRI Imaging Characteristics with Gene Expression Profiles in Renal Cell Carcinoma

**Essmaeel H. Abdel-Dayem¹, Stephen Pautler², Jonathan Walker², James R. Vasselli²,
Michael V. Knopp¹, Richard M. Klausner², W. Mareston Linehan², and Peter L. Choyke¹**

Diagnostic Radiology Department, Warren Grant Magnuson Clinical Center¹

and the Urologic Oncology Branch, National Cancer Institute²,

National Institutes of Health, Bethesda, Maryland

Introduction:

Multiple clinical studies have correlated the degree of tumor vascularity on histopathology to disease progression and patient prognosis. These studies have important implications for clinical care. Imaging techniques designed to evaluate angiogenesis will aid in the characterization and staging of tumors, and with the advent of anti-angiogenic treatments, will help the clinician choose optimal treatments and evaluate tumor response. Before this can become a reality, imaging phenotypes must be correlated with histopathology and gene expression. Dynamic Contrast Enhanced MRI (DCE-MRI) has been shown to be a useful method for imaging tumor vascularity. For this reason we have undertaken a pilot study to identify differentially expressed genes between areas of high and low enhancement on DCE-MRI in human renal cancers.

Methods:

Patients with sporadic renal cell cancers scheduled for nephrectomy at the NIH Clinical Center received pre-operative DCE-MRI to evaluate tumor vascularity. Areas of high and low contrast enhancement were selected by a staff radiologist for immediate post-surgical tissue procurement. The tumors were bivalved post-operatively and the areas of the tumor correlating to the areas selected on the DCE-MRI study were collected. mRNA from the samples was isolated for cDNA microarray analysis and qRT-PCR. Immunohistochemical staining for VEGF and CD31 was also performed.

Results:

Statistical analysis of paired enhancing and non-enhancing samples from the same tumor using a Wilcoxon matched pairs signed rank test identified 242 of 8579 genes as most significantly different between the two groups. Due to the sample size, the highest tier of significance had a p-value of 0.0625. Among these genes are VEGFB, a known angiogenic factor, and HIF 1 α , a gene intimately involved in oxygen sensing and implicated in Von-Hippel Lindau (VHL) disease, the most common hereditary form of renal cell carcinoma. Also of interest, 11 ribosomal genes were contained in the list of 242 genes (4.5%) as compared to 0.4% ribosomal genes on the entire microarray chip, 11.4 times the expected number by chance alone. This higher percentage of ribosomal proteins along with the presence of several genes involved with glucose metabolism may indicate a state of increased translational activity and metabolism in the enhancing areas of the tumor. Immunohistochemical staining for VEGF and CD31 showed no correlation

with contrast enhancement profiles. qRT-PCR analysis showed increased VEGF expression in the enhancing regions of tumors in 4 of 5 cases studied.

Discussion:

In summary, DCE-MRI appears to have the most utility as a general method of monitoring functional tumor vascularity and cellular metabolism rather than a means of monitoring specific molecular events. The initial results of this pilot study are promising and merit expansion of the study to include more patients. There will need to be some modification of the protocol to address some of the obstacles inherent in working with human tissue. This experimental paradigm is important in bridging the gap between imaging technology and studies correlating histopathology with prognosis and identifies potential pitfalls in this process.

ACKNOWLEDGEMENTS:

To my mother who sacrificed so much so that I would not have to.

To my father who always kept his promise.

To my sister who has shown me the beauty of a family.

To my friends with which I have explored the love of life and learning.

To my mentors at Yale and beyond who have helped me follow my dreams.

I would like to thank Peter Choyke, W. Mareston Linehan, David Cheng, James Vasselli, Jonathan Walker, Steve Pautler, Nick Costouros, Betty Wise, Ray Tabios, and Andra Mariotti for their support and mentorship. I would also like to thank the staff and trustees of the Foundation for the NIH for their financial and educational support.

TABLE OF CONTENTS

I.	Introduction.....	1
II.	Statement of Purpose and Hypothesis	11
III.	Methods.....	13
IV.	Results.....	19
V.	Discussion.....	24
VI.	Figures.....	30
VII.	References.....	38

INTRODUCTION

The revolution in molecular and cellular biology, the unraveling of the human genome, the ability to decipher the molecular pathways that belie many of the diseases that plague humanity today have changed the manner in which we practice medicine. With this explosion of information regarding the molecular basis of disease, a need has emerged to develop non-invasive, high resolution methods to image these processes. In vivo molecular imaging has been identified by the National Institutes of Health and the medical research community at large as a unique opportunity not only to study diseases non-invasively at the molecular level, but also to help translate bench top research into clinical advances in diagnosis, management, and treatment. Molecular imaging techniques designed to advance biomedical research today, may become the diagnostic modalities of tomorrow. With substantial funding now available in this budding field, investigators from many different disciplines including molecular biologists, imaging scientists, medical physicists, combinatorial and organic chemists, and clinicians from almost all specialties have come together to help realize the promise of this endeavor.

At present, our diagnostic assessment of disease is based on anatomic or physiologic changes that are often a late manifestation of the molecular changes that underlie disease. Direct visualization of these molecular events has the potential to directly affect patient care by allowing much earlier detection of disease. It may be possible to image molecular changes in the pre-symptomatic or even pre-disease state which would allow us to intervene at an early stage when we are more likely to provide

effective treatment that can change the outcome. By directly imaging the underlying alterations of disease, we may also potentially be able to directly image the effects of therapy and, consequently, play a direct role in determining the effectiveness of treatment shortly after the initiation of therapy. An important corollary to this is that this type of work lends itself to the discovery of new molecular targets for improved and more specific treatments and imaging reagents. Of all the molecular processes that imaging scientists have attempted to detect and monitor *in vivo*, perhaps the most studied is angiogenesis.

Imaging Angiogenesis

Angiogenesis is a complex process critical to the growth and metastasis of malignant tumors. The term angiogenesis was first used to describe the growth of endothelial sprouts from preexisting postcapillary venules, but in more recent literature, the term has been used to describe the maturation of primitive vascular networks into more complex ones. Angiogenesis occurs physiologically during embryonic development, the female reproductive cycle, wound healing, and hair growth. In 1971, however, Folkman et al. proposed that tumor growth and metastasis are angiogenesis dependent processes, and that blocking angiogenesis could be an effective strategy to arrest tumor growth.¹ In 1976, Gullino et al. showed that cells in pre-cancerous tissue acquire angiogenic capacity on their way to becoming malignant tumors.² The development of these concepts prompted an intensive search for pro- and anti-angiogenic molecules. The idea of the “angiogenic switch” is now widely accepted and that the

relative amounts of pro-angiogenic and anti-angiogenic molecules determines whether or not the chemical balance is tipped towards or away from angiogenesis.

The emergence of angiogenesis as an important target for cancer therapy has led to an increased research effort targeted at understanding the mechanisms underlying the development, maintenance, and destruction of tumor vasculature. With the evaluation of numerous anti-angiogenic agents in clinical trials, the adaptation and validation of molecular imaging techniques for monitoring angiogenesis has been in great demand. The need for surrogate markers to evaluate drug effects has been highlighted by studies involving tumors with very gradual regression rates where treatment response can only be seen after several months.^{3 4} It is clear that imaging physiologic or molecular markers may be the best method to evaluate response. Several imaging techniques, in particular functional MR imaging, nuclear, and optical techniques are available for studying the angiogenic state of tumor microvasculature.

Several approaches to imaging angiogenesis have been based upon specific imaging probes to markers expressed on the altered nonendothelial surface of tumor vessels.⁵ Since these markers may also represent the targets of new treatments, it is an ideal imaging scenario. The utility of imaging at the same target is clear and may allow for the earliest target assessment possible. This is important since noticeable effects at this level may predate phenotypic effects by up to weeks or months. Unfortunately, due to practical limitations with signal to noise and imaging molecule delivery, the implementation of angiogenesis directed molecular imaging might not extend beyond highly specialized clinical trials. In this light, imaging modalities that evaluate angiogenesis at a functional level may prove to be more feasible.

Dynamic Contrast Enhanced MRI (DCE-MRI)

Magnetic resonance imaging can be used experimentally to characterize microvasculature and provide information about tumor microvessel structure and function. While it is possible to use MR imaging probes directed towards targets involved in angiogenesis, most MR modalities in use give functional information about the angiogenic state in a tissue of interest. In general these techniques rely on first pass or equilibrium contrast media enhancement. Physiologic parameters that can be extracted through pharmacokinetic modeling include flow, perfusion, permeability, and vascular structure.

MRI methods of assessing vascular characteristics have a number of advantages over other imaging modalities such as positron emission tomography (PET), single photon emission computed tomography (SPECT), and ultrasound (US). MRI is more readily available than PET and specialized ultrasound equipment. It is minimally invasive and does not involve radiation exposure. Data acquisition is quick and can be incorporated into routine imaging studies. Furthermore, MRI maintains the highest potential spatial resolution of the listed imaging modalities and is sensitive to a number of different contrast mechanisms including blood flow, microvessel permeability and size, tissue hypoxia, and metabolism. These studies when integrated can offer a more detailed picture of the tissue microenvironment.

MR techniques can be classified as nonenhanced and contrast media enhanced methods.⁶ The second group can be subcategorized based on the type of contrast medium utilized. The first category is low molecular weight agents (<1000 Da) that rapidly

diffuse into the extracellular fluid space (ECF). The second utilizes high molecular weight contrast agents (>30,000 Da) intended to be retained in the intravascular space due to their low propensity to diffuse out into the ECF. For these reasons, these contrast agents are also called macromolecular contrast media (MCMM) or blood pool agents. The final category involves contrast agents engineered to accumulate at sites of high concentrations of angiogenesis mediating molecules. These are highly specialized contrast agents that are currently under development and it will be some time before they are available for clinical trials.

Of the types of contrast media mentioned here, low molecular weight agents have been studied the most and have been utilized in multiple animal and clinical studies. This experience has helped us understand the kinetics of this type of contrast agent against the backdrop of several underlying pathophysiological processes. This knowledge is critical for the proper application of functional angiogenic imaging and the standardization of kinetic parameters for purposes of reporting.

Pathophysiologic Basis for Contrast Enhancement

As previously stated, studies have shown that the ability of some tumors to switch on the angiogenic process is an essential step towards tumor growth and metastases. The low molecular weight contrast agents used in dynamic MR act as makeshift probes for tumor angiogenesis. The contrast agent travels through the vascular system, reaches the neoplastic tissue bed, and begins to extravasate from the tumor vasculature, accumulating in the extracellular space of the tissue and subsequently rediffuses back into the vascular system with eventual elimination by the urinary system. It is postulated that contrast

agents cross permeable tumor vessels via cell structures termed vesiculo-vacuolar organelles (VVOs).⁷ VVOs are clusters of interconnecting uncoated vesicles and vacuoles that can span the thickness of vascular endothelium in a tumor providing a potential “pore” in the vascular endothelium. The characteristic increase in tumor vascular permeability is most likely attributable to the upregulation of VVO function. To support this idea, vascular endothelial growth factor staining has been observed in the VVOs of tumor associated microvascular endothelial cells.⁸

The correlation between the intensity of enhancement and the leakiness of this pathological vasculature is essential to the clinical utility of DCE-MRI. This observation has been made by several groups of investigators who showed that the intensity of enhancement is related to the vascular density within the tissue.⁹ Differences in the contrast enhancement pattern have also been shown to correlate with specific histopathological properties of tumors.¹⁰ Histological studies have found that microvascular density determined by CD31 staining was higher in malignant tissues than in normal parenchyma, but that there may also be an overlap with benign lesions, in particular inflammatory and proliferative processes.^{11 12} Certain vascular permeability factors have also been implicated as additional explanatory factors that can determine MR signal enhancement. In a study by Knopp et al, MR vascular permeability, measured as the efflux rate constant (k_{21}), closely correlated with tissue vascular endothelial growth factor (VEGF) expression, a potent vascular permeability factor.¹³ In this study, breast tumors without significant VEGF expression showed a linear correlation of k_{21} and microvessel density (MVD). Once tissue VEGF staining became more prominent, k_{21} increased rapidly, independent of MVD. In a similar histological study involving cervical

cancer, Knopp et al. were not able to show this same correlation between k_{21} and VEGF staining, but instead showed a correlation with MVD regardless of the level of VEGF expression.¹⁴ While the results of these studies are somewhat discordant, the role of the VEGF family of genes in determining microvascular permeability is supported by several studies showing reductions in kinetic parameters after treatment with antiangiogenics including VEGF tyrosine kinase inhibitors in humans.¹⁵ While the list of modulators of angiogenesis grows, it is clear from these studies that functional angiogenic imaging can not only help validate studies of angiogenic and anti-angiogenic agents, but may help in the identification of new molecular targets for treatment.

Standardization and Quantification of DCE-MRI

The utility of DCE-MRI is increased by the fact that it can be performed on a standard 1.5 T clinical MRI system. The most important criterion for this imaging protocol is that there be a verified linear relationship between concentration of contrast media and signal intensity. After this relationship is established, the quality of the imaging protocol lies in a trade-off between spatial and temporal resolution. It is important that the temporal resolution be fast enough to detect several imaging points during the initial pass of contrast media through the tissue bed. A good guideline for this is that at least three 3-dimensional volumes should be acquired during the administration of the contrast agent when first pass kinetics are being visualized. This can be accomplished either by shortening the acquisition time by sacrificing spatial resolution, or by lengthening the duration of the contrast injection. Another important consideration is the establishment of a baseline for the determination of time intensity curves. This can

be achieved by acquiring several volumes before contrast administration. This will later allow greater reliability in the quantification of contrast enhancement. Finally, it is important that the total acquisition time be sufficiently long. While the determination of this time is related to the speed of contrast administration, it is also a function of the pathophysiological enhancement characteristics of the target tissue. Extended imaging is needed to assess the contrast washout characteristics of the tissue, which can help differentiate between malignant and benign masses. For this reason, long acquisition times (at least 5 times the length of the contrast administration time) can greatly enhance the utility of the study. It is also useful to examine contrast enhancement of some of the major arteries within an image to help establish the quality of the contrast injection. The arterial enhancement pattern can be used to verify the timing and dosage of a contrast injection and can also be used as an *in vivo* standard or an “input function” to relate tissue enhancement with contrast administration.¹⁶

Once the images are collected, the next step is to select regions of interest and create time-intensity curves for contrast enhancement. While the shape of these time-intensity curves can provide a great deal of information about the tissue of interest, they are extremely sensitive to patient motion. The motion of tissue in and out of the plane of the slice can affect the validity of the generated curve. For this reason, patient positioning, proper volume selection, and the use of positioning devices and compression belts can greatly increase the quality of the study.

There are three features that should be considered in any time-intensity curve: the initial rate of enhancement (k_{21}), the time and intensity of the peak enhancement or amplitude of the curve (A), and the washout or contrast elimination after peak

enhancement (k_{el}).¹⁷ Pharmacokinetic modeling, in our case a two compartment model proposed by Brix et al, is used to help relate these quantitative parameters with physiologic concepts (figure 3).¹⁸ These models can be used to overlay calculated parameter images over high-resolution two-dimensional images to generate color-encoded maps of tumor perfusion and vascular permeability. This is particularly important in these types of studies because of the large numbers of images generated that would be extremely time consuming to analyze without the aid of parameter maps (figure 4).¹⁹ These parameter maps not only simplify the analysis of this data, but also render this data readily shared between clinicians.

Clinical Applications

Because DCE-MRI can be performed on most clinical strength magnets and requires no special equipment, it has lent itself to investigation in multiple clinical studies. Perhaps the most promising application for this modality is in lesion characterization. Observations from multiple studies have shown that malignant tissues generally have a steep, high intensity curve expressed mathematically by a high k_{21} . This has been studied most extensively in the breast and, subsequently, DCE-MRI may eventually have a role in screening patients at high risk for breast cancer. However, because there is an overlap between the enhancement patterns of benign and malignant breast lesions, the sensitivity of breast MRI may be high, but the specificity may not be as good.²⁰

Contrast enhancement patterns on dynamic imaging have also been shown to predict prognosis. In patients with cervical cancer, it was observed that tumors with a

rapid initial rate of enhancement were more likely to carry a poorer prognosis for patients despite exhibiting a better response to radiotherapy.²¹

DCE-MRI can also help predict or monitor the effects of a number of different treatments. Studies have been performed looking at DCE-MRI in the neoadjuvant chemotherapy of breast cancer and sarcomas of the bone. For example, in breast cancer, it has been found that a decrease in vascular permeability can be seen with a response to chemotherapy, and that the absence of a decrease in permeability after only 1 or 2 cycles of treatment can predict a treatment nonresponder.²² A number of studies have also reported on the utility of DCE-MRI in monitoring the effects of anti-angiogenic therapies. In these studies, a successful response to therapy resulted in a decrease in tumor enhancement whether it was evaluated in a quantitative or a semi-quantitative fashion.^{23 24}

Tumor response to therapy as measured by DCE-MRI is relatively non-specific to treatment modality. This observation may indicate that tumor cell kill, no matter how it is achieved, should ultimately result in vascular compromise. While this allows DCE-MRI to be used to assess treatment response at an early stage, it may mean that it is limited in its ability to indicate to us the process at the source of the tumor response. Still, the observation of the phenotype of vascularity and changes in this phenotype can help us design experiments to search for the molecular changes associated with it. DCE-MRI as a phenotypic measurement of vascularity can help us direct not only a targeted search, but also genome wide screening for novel genes regulating tumor angiogenesis and response to therapy.

STATEMENT OF PURPOSE AND HYPOTHESIS

Clinically there have been a number of studies relating the degree of vascularization on direct tissue examination to tumor progression and patient prognosis.²⁵ These studies have important implications for clinical care. Functional characterization of tumor neovasculature can aid in tumor detection, characterization, and staging. Furthermore, with a multitude of anti-angiogenic therapies in clinical trials, imaging techniques designed to evaluate angiogenesis can help the clinician choose the most appropriate treatment, optimize the treatment dose, and detect early responses or failures. Further clinical implications include the identification of angiogenic molecular targets within tumors and the possible development of individualized image based drug delivery systems. Still, before this can become a reality, functional imaging phenotype must be correlated with histopathology and gene expression.

As stated previously, several studies have attempted, some successfully to validate dynamic T1-contrast enhanced MR kinetic parameters with markers of angiogenesis in human tumors. In general, these studies have looked at differences between patients with tumors exhibiting different patterns of contrast enhancement. In our experience, we have found many tumors to be extremely heterogeneous in nature, with parts of a single tumor showing high levels of contrast enhancement while others showing very little enhancement at all. This observation raises the question as to whether or not these areas exhibiting different MRI contrast enhancement phenotypes within the same tumor are differentially expressing angiogenic genes that are soliciting neovascularity. If this is the case, there should be differential gene expression when

examining these different areas of the same tumor. This would have important implications for the classification of tumors through biopsies since biopsies in many cases only sample a small amount of tissue within a tumor that may not be exhibiting malignant features. This type of functional microvascular imaging may help direct tissue sampling for more accurate clinical prognoses and for purposes of tissue procurement in angiogenesis research.

To address this question, we have undertaken a pilot study of kidney cancers using pre-operative Dynamic Contrast Enhanced MRI (DCE-MRI) followed by procurement of tumor tissue from areas with different enhancement characteristics within the same tumor. The samples were run on cDNA microarrays to identify differences in gene expression profiles between enhancing and non-enhancing regions (figure 1).

Hypothesis:

Areas of high and low enhancement on Dynamic Contrast Enhanced MRI (DCE-MRI) of renal cell carcinomas have differentially expressed genes that can be identified by cDNA microarray analysis.

METHODS

Clinical Material.

Subjects for the study were chosen from amongst patients receiving their care at the NIH's Urologic Oncology Branch for sporadic renal cell carcinoma. Patients who were to receive total nephrectomies were consented and scheduled for pre-operative dynamic contrast-enhanced MRI 1-2 days prior to total nephrectomy. All nephrectomies were performed at the National Institutes of Health Clinical Center by urologists in the Urologic Oncology Branch of the National Cancer Institute.

Dynamic Contrast Enhanced Magnetic Resonance Imaging

Imaging was performed using a 1.5 T clinical imaging system (GE medical systems, Milwaukee, WI). The dynamic portion of the abdominal MR imaging protocol included a static 3D-FSPGR pre- and post-contrast acquisition followed by a dynamic image series which was acquired coronally as 23 volumes each containing 12 - 4mm slices through the kidney of interest with 30 seconds between the start of each volume acquisition (TR = 7.8, TE = 4.2, Flip = 25°, NEX = 0.5, 256 x 192 matrix). Patients were asked to hold their breath for 15 seconds while the image was acquired and were allowed to breathe for another 15 seconds before the start of the next cycle. The coronal view was chosen for easier correlation of the imaging data with the gross specimen post-surgically and because it posed fewer problems with motion artifacts from inconsistent breath holding during acquisition. After three to four volumes were acquired to establish a baseline, 0.1mmol/Kg Gadolinium-diethylene triamine pentaaceticacid (Gd-DTPA) was

injected slowly over the course of 1 minute and the flow of contrast was followed out for the remainder of the 10-minute scan (figure 2).

Contrast enhancement was quantified using a two compartment model described by Brix et al. that describes the enhancement as a the parameter amplitude (A), redistribution rate constant (k_{21} [min^{-1}]), and elimination rate constant (k_{el} [min^{-1}])²⁶ Using this model, pharmacokinetic analysis was performed using in house software written for IDL (author MVK). Time-intensity curves were generated for different regions of interest (ROIs) and were fitted to the pharmacokinetic model. The maximal amplitude of enhancement the tissue exchange rate constant (k_{21}) were calculated for each pixel and were color coded to assist in the visualization of these parameters within the tumor (figure 3). Based on these parametric maps and cinematic views of the tumor during contrast enhancement, areas of high and low enhancement were selected by a staff radiologist for tissue procurement immediately post-operatively.

Tissue Procurement

Post-surgically, the tumors were bivalved and photographed to demonstrate correlation between the imaging and the pathology before the previously selected regions of the tumor were excised and frozen immediately in OCT compound. When excising the selected regions of the tumor, care was taken to stay away from regions of gross necrosis and to select areas that looked grossly viable. A sample of normal kidney was also procured at this time and banked for future study.

Microarray Procedures

Total RNA was isolated from the tumor samples by grinding the tissue fragments into fine powder by mortar and pestle on dry ice, and homogenizing the powder in 5 ml of TRIzol (Gibco BRL, Gaithersburg, MD). While this procedure yielded ample amounts of a full range of RNA species as verified by gel electrophoresis, this total RNA resulted in low signal intensities and an unacceptable amount of non-specific background. This was most likely due to a low ratio of mRNA to ribosomal RNA. For this reason, messenger RNA was isolated from total RNA with a Micro-Fastrak 2.0 kit (Invitrogen, Carlsbad, CA) to improve the signal to noise ratio. Only very small amounts of mRNA could be obtained from the total RNA using this process. For this reason, an amplification step was added to maximize the signal intensity and reduce the amount of non-specific background on the microarrays. Linear mRNA amplification has been shown to improve the quality of cDNA microarrays without compromising the fidelity of the original mRNA species isolated from the tumor.²⁷

In the amplification step, the mRNA was reverse transcribed (RT) by priming with oligo-dT, into single stranded DNA and double stranded DNA transcribed from a primer added during the RT reaction.²⁸ One round of in-vitro transcription amplified approximately 2ug of mRNA into 30 – 100ug of amplified mRNA. The amplified tumor and normal mRNA were reverse transcribed incorporating a Cy3 (Green) labeled thymidine into the newly formed DNA molecule. All tumor and normal DNA was hybridized against a standard reference consisting of amplified mRNA from 6 pooled tumor cell lines labeled with Cy5 (Red) onto the NCI 9,600 oncogene chip using the Stratagene Fairplay® microarray kit.

Data Analysis

The microarrays were scanned using a GenePix 4000 microarray scanner (Axon Instruments, Foster City, CA) and analyzed using GenePix Pro 3.0 software. Spots were excluded if there was an obvious problem with the hybridization or if the spot was defective. Log base 2 -ratios of local background subtracted intensity levels were analyzed. Log ratios were considered missing for spots with intensity less than 50 in both channels (truncated at ± 6) and if less than 50% of spots were not at least 1 SD above background. A spot was filtered out from analysis if the log-ratio was missing in more than 30% of the arrays. Log-ratios for each microarray were median centered to adjust for dye bias and PMT settings.

The arrays were then loaded and stored in a database supported by the Center for Information Technology at the National Institutes of Health. Statistical analysis was performed with software developed by the National Human Genome Research Institute (Bethesda, MD). The arrays were categorized as enhancing or non-enhancing and a Wilcoxon Matched Pairs Signed-Rank test was run to compare data in the two groups. This statistical test allowed the arrays to be analyzed in pairs from the same patient, looking for differences in expression levels that are consistent across the patient population while maintaining an internal control to cancel out normal variations between individual patients.

Immunohistochemical staining for VEGF and CD31

We performed immunohistochemical studies on 5 tumor pairs selected for the quality of their imaging studies and microarray data. All samples were acquired immediately post-operatively and frozen in OCT compound. The samples were cut in 6 μm sections and stored on slides at -80°C for staining. The tissue sections were stained with VEGF and CD31 rabbit polyclonal antibodies (Dako, Carpinteria, CA) at 1:200 dilution. Sections for immunostaining were treated with 3% hydrogen peroxide for 10 minutes to quench myeloperoxidase and then cleared in running water followed by a 5-minute rinse in Tris-buffered saline (TBS) at a pH of 7.6. Slides were mounted on the Dako Autostainer and incubated with antibody to VEGF (1 hour) and staining was completed using the Dako Rabbit Envision Plus Kit (Dako, Carpinteria, CA). The sections were removed from the stainer and counterstained with a modified Mayer hematoxylin followed by 10 dips in 0.3% ammonia water. Sections were rinsed in running tap water and mounted with Immunmount (Harvey Instruments, Buffalo, NY). Negative controls were run containing no antibody. Two sections through each tumor were stained in this manner, and the degree of staining was assessed by a staff pathologist at the NIH Clinical Center using a 0 to 3 scale with 3 being the strongest level of staining.

Quantitative Real-Time PCR (qRT-PCR) of tumor VEGF

qRT-PCR analysis was performed on the five tumor sets that were analyzed by microarray. cDNA from the reverse transcription step of RNA amplification was banked and used for the qRT-PCR studies. Primers and probes for VEGF were the standard VEGF set from Applied Biosystems (Foster City, CA). β -actin was amplified in the same

tube with VEGF as a control and was used for purposes of normalization. Primer and probe sets for β -actin were also supplied by Applied Biosystems. Real time PCR reactions for all samples were conducted in a volume of 25 μ L using the Taq-Man qRT-PCR kit (Applied Biosystems, Foster City, CA). Thermal cycler parameters were 2 minutes at 50°C, 10 minutes at 95°C, and 40 cycles each consisting of a 15 second denaturing step at 95°C and a 1-minute annealing step at 60°C. All assays were performed in duplicate or triplicate and the results reported as the mean. Standard curves were generated and the relative expression levels normalized to β -actin levels for each sample.

RESULTS

Dynamic Contrast Enhanced MRI:

A total of 10 patients were imaged between 8/16/2001 and 7/2/2002. Two of the patients were excluded due to inadequate imaging exams, one was excluded due to the high degree of necrosis at the time of tissue procurement, and two were excluded due to insufficient amounts of RNA extracted for cDNA microarray. This left tumors from a total of 5 patients that were successfully microarrayed.

All 5 cases showed heterogeneously enhancing tumors with distinct pharmacokinetic regions within each tumor. Examples of two DCE-MRI studies are shown in figures 5 and 6 along with the correlation of the image with the gross specimen for tissue procurement.

Microarray Analysis and mRNA Expression Profiles

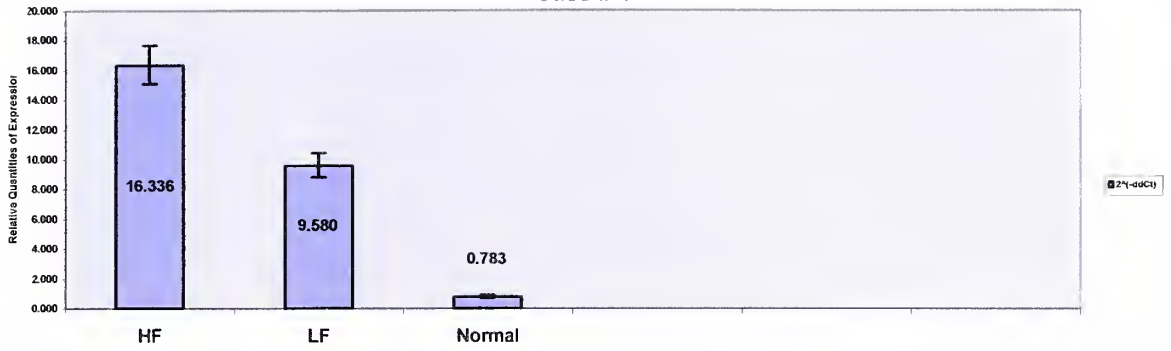
Microarrays were successfully performed on 5 patients, 4 with clear cell renal cell carcinoma, and one with a collecting duct tumor. The quality and reproducibility of the arrays was verified through scatter plots and multidimensional scaling. Three samples were run in duplicate to check for reproducibility of arrays and the Pearson correlation coefficient for these samples on scatter plots were all $>.90$. The initial evaluation of the tumor sets was done by scatter plot analysis to show outlying genes (Figure 7) before evaluation with a Wilcoxon test. From the complete set of printed genes, 8,579 passed the baseline quality control filtering criteria for spot size, intensity, signal to noise, and presence in greater than 70% of the arrays. Wilcoxon match pairs signed rank test

analysis identified 242 out of 8579 genes as the most significantly different between the two groups. Due to the small sample size and the nature of the statistical analysis, the 242 genes identified as having the greatest significance could not achieve significance below a p-value of 0.0625 (Figure 8). Among these genes are VEGF B, a known angiogenic factor, and HIF 1 α , a gene intimately involved in Von-Hippel Lindau Disease (VHL) which is the most common form of hereditary RCC. Both of these genes are potential prognostic markers for RCC and they are upregulated in the enhancing areas. Vascular endothelial growth factor was not filtered out as differentially expressed in this set of genes. Also of interest, 11 ribosomal genes were contained in the list of 242 genes (4.5%) as compared to 0.4% ribosomal genes on the entire microarray chip, 11.4 times the number expected by chance alone. This higher percentage of ribosomal proteins along with the presence of several genes involved with glucose metabolism may indicate a state of increased translational activity and metabolism in the enhancing areas of the tumor.

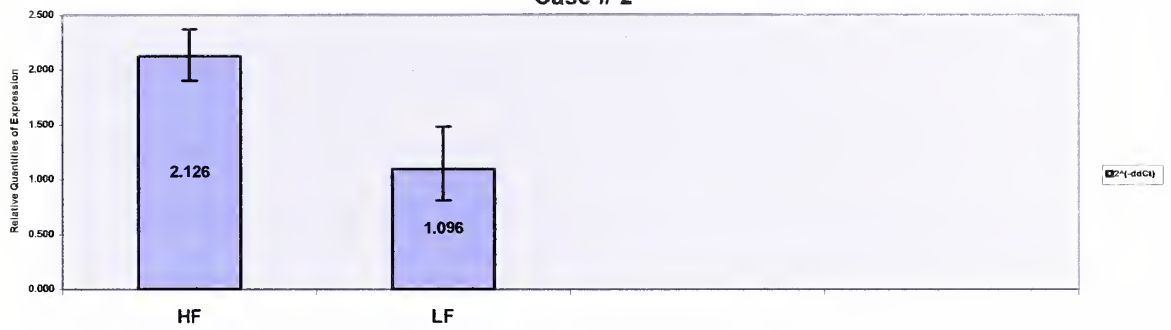
RT-PCR Analysis of VEGF Expression

When enhancing and non-enhancing samples were compared with regard to VEGF expression as evaluated by RT-PCR, 4 of the 5 cases studied showed statistically greater VEGF expression in the enhancing sample over the non-enhancing sample. The results of these experiments are shown in the graphs below. While this data may be suggestive of an increase in VEGF expression in enhancing areas, the low sample number does not allow for the establishment of statistical significance.

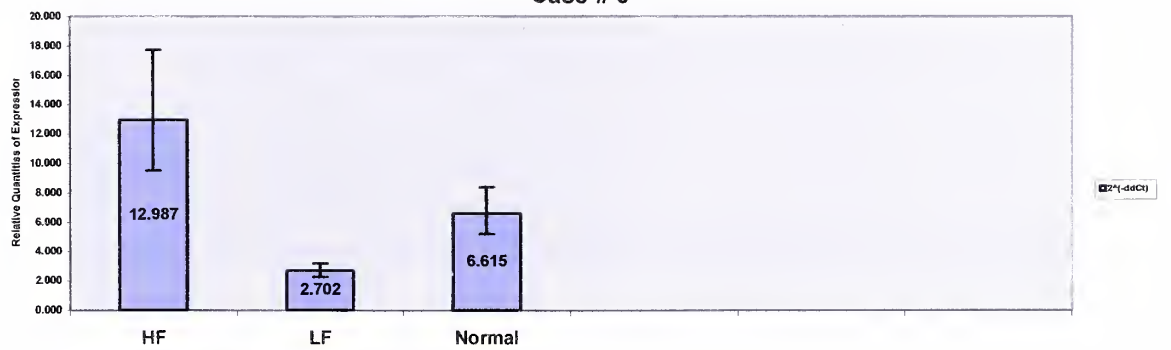
Case # 1



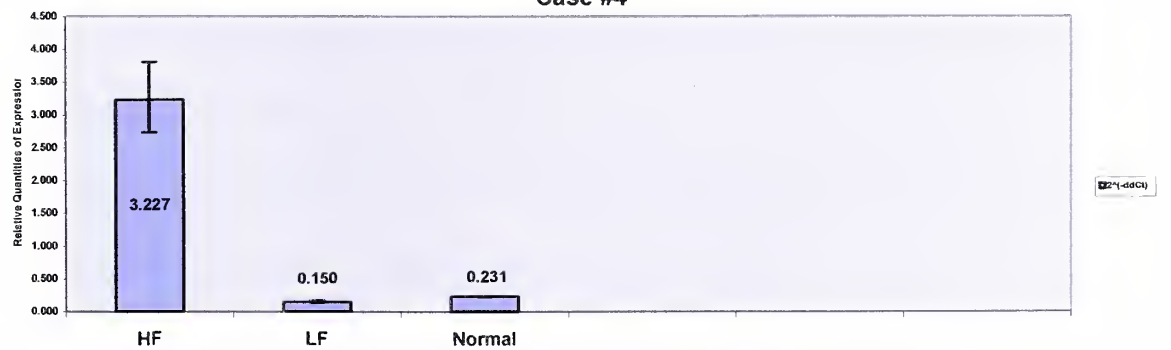
Case # 2



Case # 3



Case #4



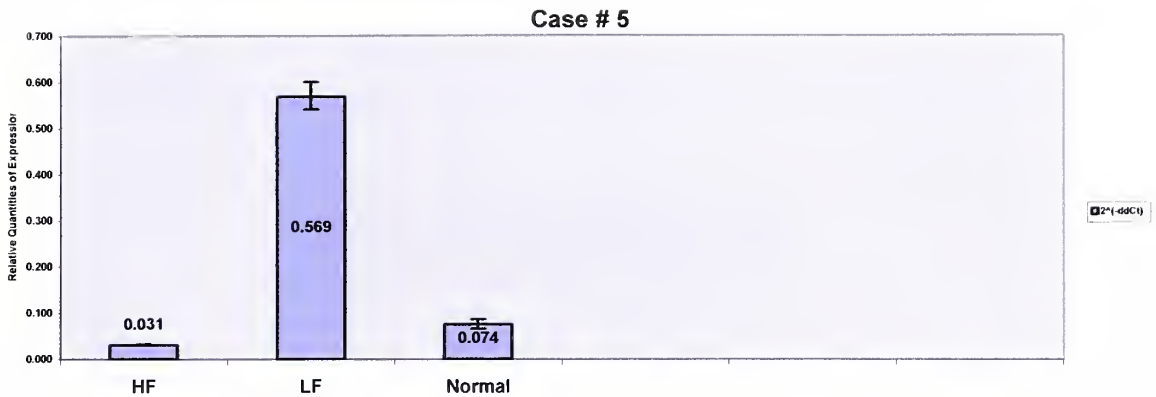


Figure 9. qRT-PCR of VEGF: Quantitative RT-PCR analysis of VEGF expression in high flow (HF) and low flow (LF) regions of renal cell carcinomas as evaluated by DCE-MRI. When possible, a sample of normal kidney was assayed from each patient for comparison. Cases 1 through 4 show increased VEGF expression in the contrast enhancing or high flow regions of the tumor while the final case shows very low VEGF expression in the contrast-enhancing region.

Immunohistochemical Staining of VEGF

Histological examination of sections stained with VEGF antibodies showed no correlation with contrast enhancement in the tumors examined. Of the 5 cases stained, VEGF staining was rated higher in the enhancing sample in 2 of the 5 cases while the non-enhancing sample showed a greater degree of VEGF staining in another 2 of the 5 cases. The last case showed minimal VEGF staining in both samples from that tumor. The results are shown in table 1. The normal kidney sample from all cases did not stain with the VEGF antibody. No difference was seen with hematoxylin staining between the enhancing and non-enhancing samples from each tumor. Furthermore no association was

seen between tissue enhancement on DCE-MRI and micro-vascular density as evaluated by CD31 staining.

VEGF Staining			
	Sample	Rating	
Case 1	HF	Focal	2
	LF	Focal	1
	Normal	Weak	0
Case 2	HF	Focal	1
	LF	Diffuse	2
	Normal	Neg	0
Case 3	HF	Focal	3
	LF	Focal	1
Case 4	HF	Neg	0
	LF	Diffuse	2
	Normal	Neg	0
Case 5	HF	Neg	0
	LF	Neg	0
	Normal	Weak	0

Table 1. Immunohistochemical staining for VEGF: Two sections through each tumor sample were stained with VEGF rabbit polyclonal antibody, and the degree of staining was assessed by a staff pathologist at the NIH Clinical Center using a 0 to 3 scale with 3 being the strongest level of staining. HF represents the enhancing or high flow sample of each tumor while LF represents the non-enhancing or low flow sample. No association is seen between tissue enhancement on DCE-MRI and VEGF staining. Similar staining with CD31 to evaluate micro-vessel density also showed no association with enhancement.

DISCUSSION

Several studies have attempted, some successfully to validate dynamic T1-contrast enhanced MR kinetic parameters with markers of angiogenesis in human tumors. In general, these studies have looked at differences between patients with tumors exhibiting different patterns of contrast enhancement. In our experience, we have found many tumors to be extremely heterogeneous in nature, with parts of a single tumor showing high levels of contrast enhancement while others showing very little enhancement at all. As DCE-MRI evolves into an important tool for evaluating tumor vasculature, the molecular mechanisms that underlie this enhancement heterogeneity must be elucidated. This information will help us determine the significance of this heterogeneity and whether or not it should be taken into account clinically when using DCE-MRI to evaluate tumors and in tissue biopsies.

To our knowledge, this study is the first attempt to look for differences in mRNA expression profiles based on intra-tumoral differences in contrast enhancement on dynamic MRI in humans. The pharmacokinetic models used in DCE-MRI assume that enhancement is dependent on the amount of functional tumor vasculature. For this reason we had initially hypothesized that variations in contrast enhancement would be dependent upon perfusion related phenomena based on the action of angiogenic factors. While this was a pilot study to conceptually test this type of experimental paradigm in humans, the preliminary results demonstrate several interesting observations and provide insight into contrast enhancement heterogeneity on DCE-MRI.

One of the most interesting findings is the disproportionately high number of ribosomal genes in our microarray analysis. These increases in ribosomal gene transcription may indicate an increased cellular demand for translational activity which is typically seen in proliferating cell populations or cells stimulated by oxygenation, nutrition, growth factors, or changes in temperature.²⁹ Thus, it is logical that areas of a tumor with greater degrees of enhancement on DCE-MRI are receiving increased oxygenation and nutrition and consequently show increased ribosomal transcription and increased cellular activity. This observation was made by Costouros et al in a similar experiment in an animal model.³⁰ In this study, DCE-MRI was performed on murine subcutaneous tumors and areas were chosen for laser capture microdissection, and genetic profiling of tumor heterogeneity based on the pharmacokinetic parameters observed. There was no evidence in this study of increased expression of proangiogenic factors at the transcriptional level in either pharmacokinetic region, and there was no difference observed between the regions on immunostaining with CD31, a measure of microvessel density. However, the expression of ribosomal proteins was found to be greatly increased in the enhancing areas implying increased protein translation and increased cellular activity. Supporting this concept in our study are several genes involved in glucose metabolism that are also upregulated in the enhancing regions of the tumors. These include hexokinase 3, insulin receptors, glucose-6-phosphate transporter gene, and pyruvate kinase. This is especially interesting considering there are studies that have correlated FDG hypermetabolism on PET with Gd-DTPA enhancing tumors.^{31 32}

The relative absence of angiogenic factors from the filtered microarray results indicates that DCE-MRI appears to be most useful in evaluating functional tumor

vasculature and cellular metabolism rather than specific molecular events. With that said, two genes from the list of 242 are particularly interesting from a molecular standpoint. Vascular endothelial growth factor B (VEGF B) is a member of the VEGF family of proangiogenic factors while hypoxia inducible factor 1 α (HIF 1 α) is an oxygen sensing gene involved in the VHL pathway, the pathway implicated in most renal malignancies. While multiple studies mentioned earlier were able to correlate VEGF expression with contrast enhancement between tumors, VEGF expression alone could not explain differences in contrast enhancement in the same tumor by immunostaining or qRT-PCR. Further work may eventually point to an angiogenic factor or multiple factors as an explanation for the observed heterogeneity within a tumor, but the relative absence of pro-angiogenic factors from our analysis may imply post-transcriptional or even post-translational modifications as an explanation. As such, proteomics may play an important role in deciphering the underlying molecular processes.

Several more tumors will need to be studied before definitive genes of interest can be identified by cDNA microarray and verified by quantitative methods such as RT-PCR and immunohistochemistry. This pilot study has however identified many potential pitfalls involved in working with human subjects that must be addressed before further expansion of this work.

As mentioned earlier, one of the major difficulties inherent in imaging the kidneys in this fashion is patient motion. DCE-MRI is exquisitely sensitive to motion in and out of the slice of acquisition over the course of 10 minutes and several cycles of breath holds by the patient. This type of artifact can greatly degrade the quality of the time-intensity curves generated from these studies. For this reason, image homogeneity and the

reduction of motion artifacts are even more critical for functional imaging than for morphologic imaging. To help minimize this problem, we switched from a transaxial view to a coronal view when acquiring images, which helped minimize motion in and out of the plane of view. While there was slightly more translational motion observed in the coronal plane, this is much easier to correct for than motion across slices. Several motion correction algorithms were used in an attempt to correct for respiratory motion with little success. While motion correction software is still not advanced enough to adequately correct these high-resolution images, the use of positioning devices, compression belts, and proper patient coaching to improve the consistency of their breath holds can substantially improve image quality.

A second consideration in this type of study is the accuracy of image guided tissue acquisition. Great care was taken to correlate the imaging study with the gross specimen at the time of tissue acquisition. All the specimens were taken from cases where the patient received a total nephrectomy. In this manner, the kidney could be grossly oriented and selected landmarks identified within the tumor. Using these landmarks, and keeping in mind the slice thickness of the MRI, the selected areas were collected for analysis. Care was taken to select the larger volumes of enhancement within the tumor to allow for error due to patient motion and human error. While this technique of image guided tissue acquisition is crude at best, it represents the best method currently available that maintains the standard of care for the patients in the protocol without subjecting them to unnecessary interventional procedures. With the advent of MR guided interventional procedures, other options include online DCE-MRI guided tissue biopsies. Several groups are working on fiducial markers that can be inserted at the time of

imaging and used for motion correction and as a landmark for tissue acquisition. This could conceptually be investigated as an adjunct to studies of interventional techniques such as radio frequency ablation (RFA).

An added benefit to online interventional tissue acquisition schemes is that there is no warm ischemia time to the organ of interest. The effect of warm ischemia on microarray data is not well understood. Huang et al. attempted to quantify the effects of warm ischemia on gene expression profiles in normal mucosa from human colon cancer specimens.³³ Their statistical models suggested that three patterns were induced by ischemia. The first group consisting of 68.2% of evaluated genes showed an average 27% increase in expression over 60 minutes from the 5-minute baseline. The second group comprising 17.8% of evaluated genes showed only an average 12% increase or decrease over 60 minutes. The final group comprising 13.4% of the evaluated genes showed the most sensitivity with an average increase or decrease of 50% over 60 minutes. It is not known exactly which genes on a given chip would belong to which group which is why it is important to keep the warm ischemia time as low as possible. Warm ischemia time in the samples in this study were estimated to be well over an hour, but because all comparisons were made within the same set of tissue, the warm ischemia experienced by all samples in a tissue set should be the same and the relative levels of RNA should be preserved. Still, warm ischemia times should ideally be cut to below 20 minutes. We are currently looking at surgical procedures developed for kidney harvesting for transplantation that would reduce the warm ischemia time by preserving the renal pedicle until near the end of the procedure.

In summary, DCE-MRI appears to have the most utility as a general method of monitoring functional tumor vascularity and cellular metabolism rather than a means of monitoring specific molecular events. While the pharmacokinetic parameters measured by DCE-MRI do not necessarily correlate with active angiogenesis, this does not undermine its utility as a marker of response to antiangiogenic therapies as has been shown in several studies mentioned earlier. In this situation, a change from a baseline study can indicate a change in the vascular status of a tumor, but may not allow us to draw conclusions about an active angiogenic process. Perhaps most importantly, in this study we have demonstrated an experimental method of investigation to help understand the underlying molecular mechanisms of imaging modalities by correlating their imaging phenotypes with in vivo molecular events. The initial results of this pilot study are promising and merit expansion of the study to include more patients. There will need to be some modification of the protocol to address some of the obstacles inherent in working with human tissue. This experimental paradigm is important in bridging the gap between imaging technology and studies correlating histopathology with treatment and prognosis. It is hoped that one day, functional tumor imaging will be able to provide the clinician with the pathophysiological data necessary to direct patient care.

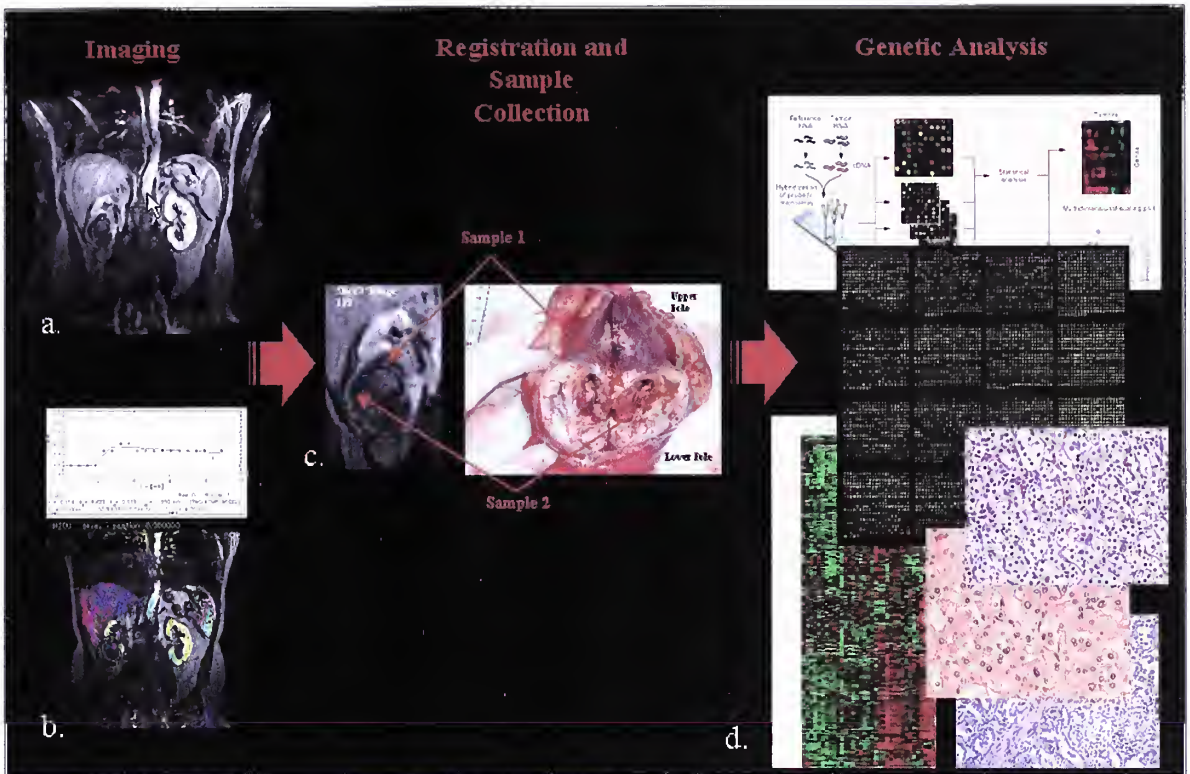


Figure 1. Experimental Paradigm: To test the hypothesis that different rates of contrast enhancement within kidney tumors reflect differences in gene expression, pre-operative DCE-MRI studies were performed on patients with sporadic renal cell carcinoma scheduled for nephrectomy (a). The images were processed and time-intensity curves were generated (b). These images were then used to guide sample procurement from areas exhibiting high or low levels of enhancement (c). Finally, RNA was extracted from part of these samples and analyzed using cDNA microarrays. A portion of the tissue sample was retained for immunohistochemistry studies and cDNA was also banked for qRT-PCR experiments.

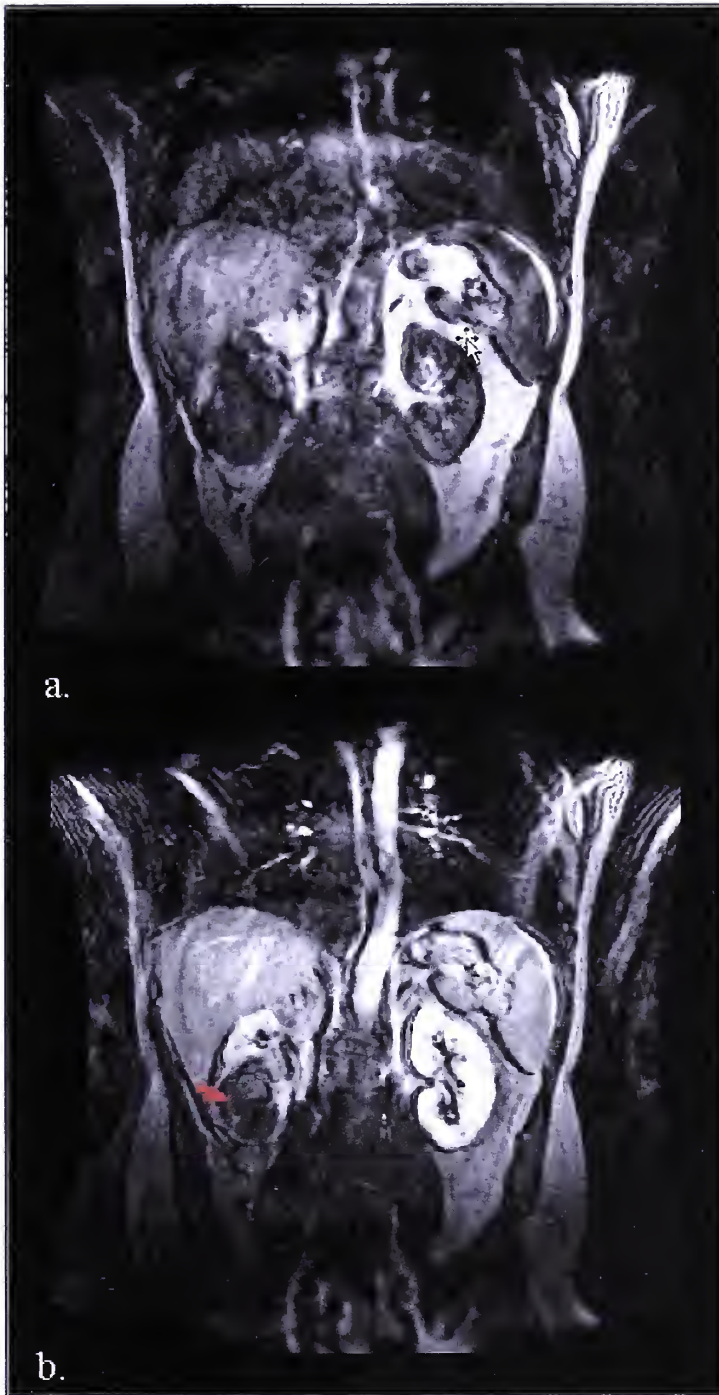


Figure 2. Dynamic Contrast Enhanced MRI (DCE-MRI): (a.) T1 weighted pre-contrast image of a patient with RCC of the right kidney. (b.) The tumor is seen to enhance differentially after a slow injection of Gd-DTPA (arrow).

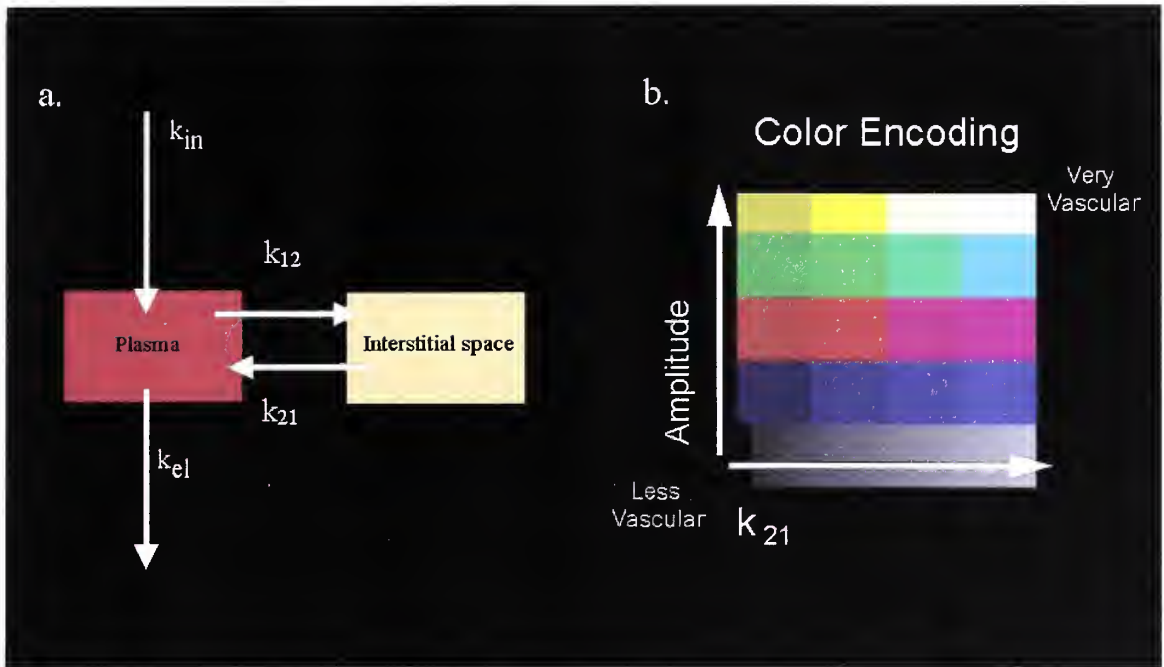


Figure 3. Pharmacokinetic Modeling: (a.) Pharmacokinetic model for contrast enhancement described by Brix et al. Enhancement here is described as a parameter amplitude of the maximal signal intensity (Λ), a redistribution rate constant (k_{21} [min^{-1}]), and an elimination rate constant (k_{el} [min^{-1}]). (b.) A 16-color pixel-by-pixel parametric color-coding scheme for amplitude and k_{21} parameters.

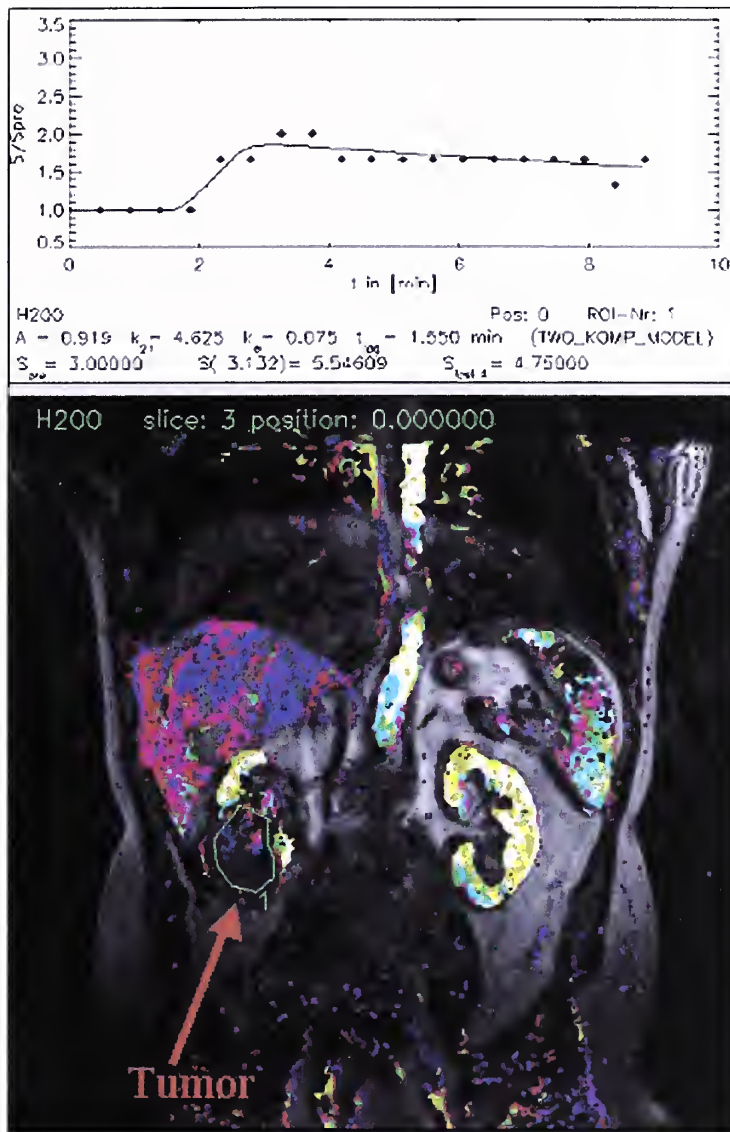


Figure 4. Parametric Mapping: Average enhancement curve of a region of interest (ROI) through the center of a renal cell carcinoma with the corresponding parametric color map. These types of images condense the large amount of data generated from DCE-MRI studies into a single image that is easily analyzed and shared between clinicians.



Figure 5 Tissue Procurement: T1 dynamic contrast enhanced study of a patient with renal cell carcinoma. Tumor heterogeneity is seen on parametric mapping of the tumor (top) and on the raw images of tumor enhancement (middle). Correlation of imaging with gross pathology is shown (bottom).

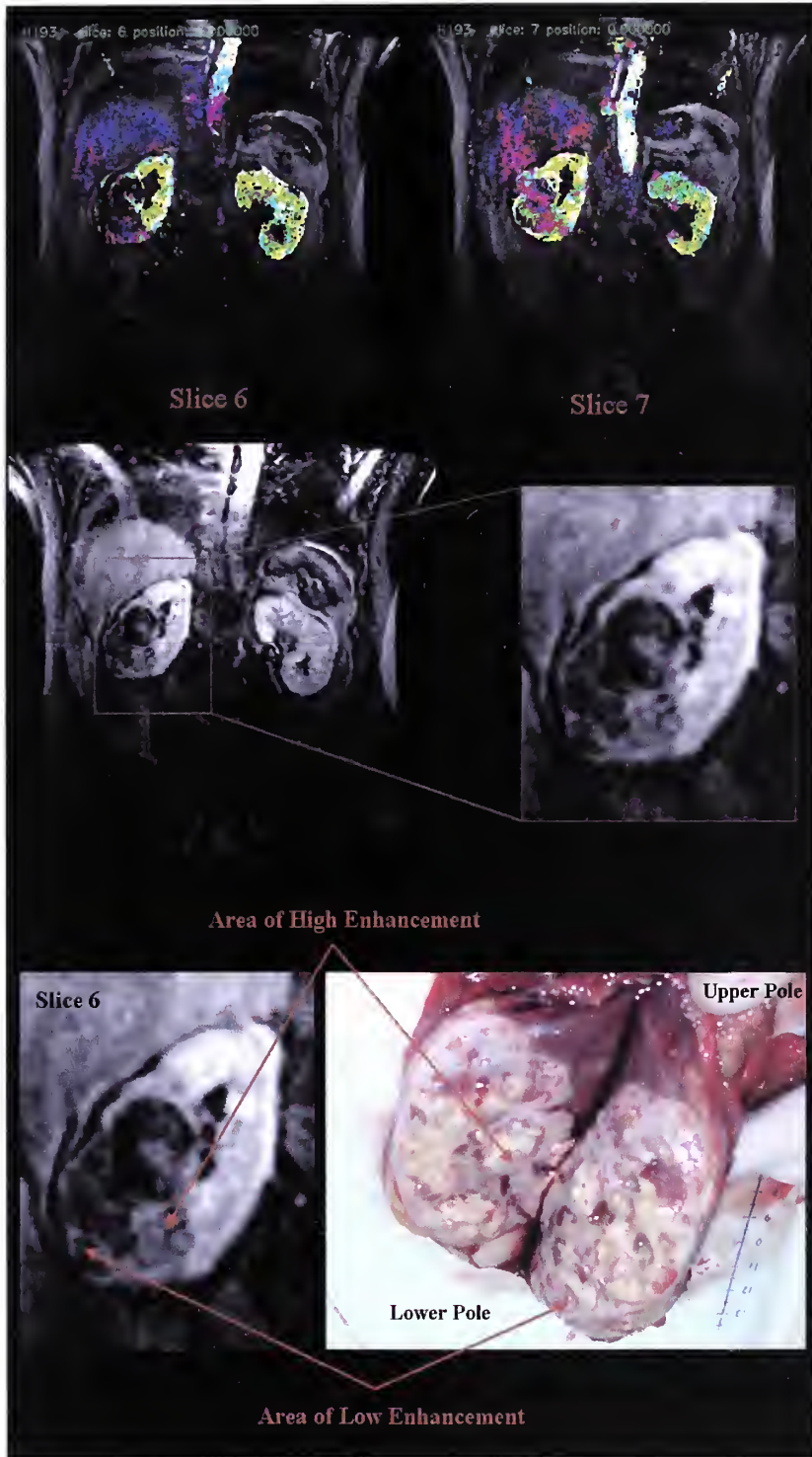


Figure 6. Tissue procurement: T1 dynamic contrast enhanced study of a patient with renal cell carcinoma. Tumor heterogeneity is seen on parametric mapping of the tumor (top) and on the raw images of tumor enhancement (middle). Correlation of imaging with gross pathology is shown (bottom).

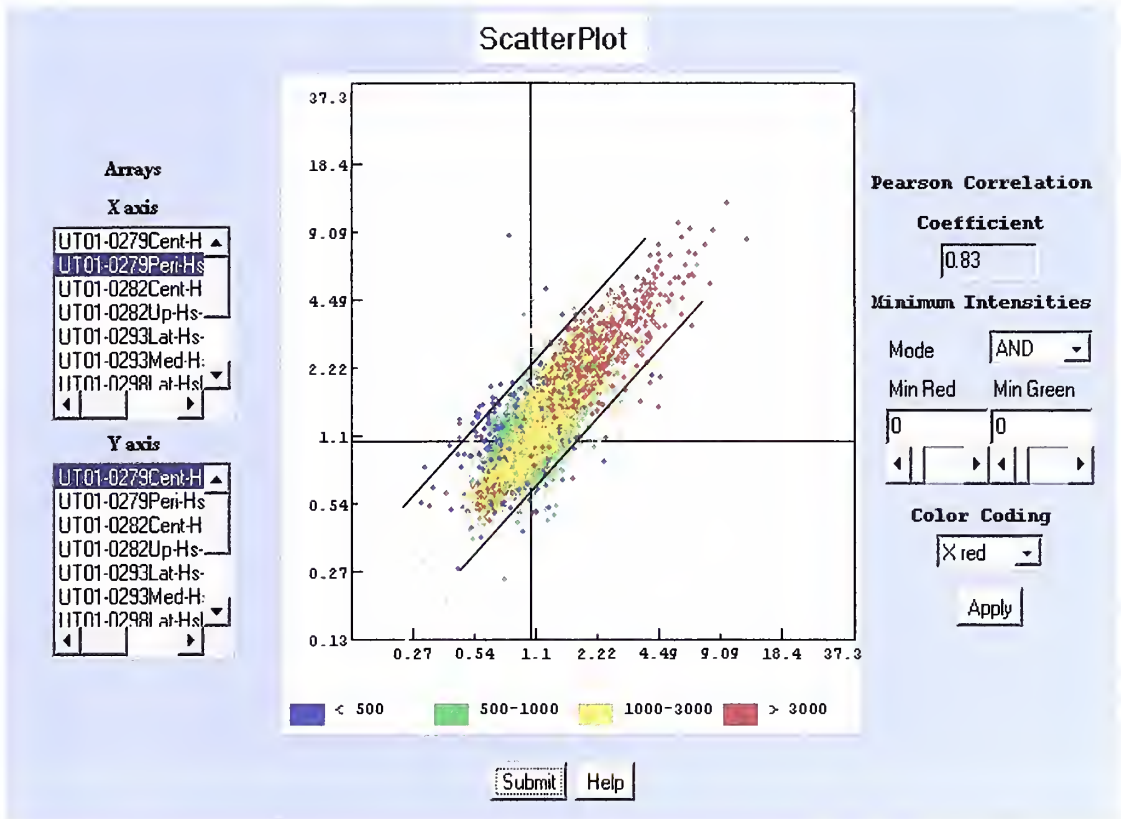


Figure 7. Scatter Plots: This example of a scatter plot shows the similarities between an enhancing (y-axis) and non-enhancing (x-axis) sample from the same patient. While the arrays appear very similar, there are several outliers beyond the parallel lines. While this analysis is useful for identifying the genes that vary the most between two arrays from the same person, it is not useful in identifying genes that vary slightly but consistently between the enhancing and non-enhancing samples from each patient. For the second type of analysis, a Wilcoxon test was used (See **Data Analysis** section).

										Gene	Difference
A	A	A	A	B	B	B	B	B	B		
#1	#2	#3	#4	#5	#6	#7	#8	#9	#10		
										VEGFB - Vascular Endothelial Growth Factor B	-0.569
										HIF1A - Hypoxia Inducible Factor 1, alpha subunit	-0.305
										HK3 - hexokinase 3	-0.303
										INSR - insulin receptor	-0.312
										G6PT1 - glucose-6-phosphate transport	-0.247
										PDK2 - pyruvate dehydrogenase kinase	0.100
										PKM2 - pyruvate kinase	-0.917
										RPL10A - ribosomal protein L10a	-0.285
										RPL12 - ribosomal protein L12	-0.075
										RPL13A - ribosomal protein L13a	-0.636
										RPL23A - ribosomal protein L23a	-0.464
										RPL37 - ribosomal protein L37	-0.417
										RPL7A - ribosomal protein L7a	-0.423
										RPS14 - ribosomal protein S14	-0.251
										RPS15 - ribosomal protein S15	-0.291
										RPS24 - ribosomal protein S24	-0.707
										RPS28 - ribosomal protein S28	-0.426

Figure 8. Analysis of cDNA microarray data: A Wilcoxon Matched Pairs Signed-Rank test was run on 8579 genes to compare levels of expression in enhancing (group A) and non-enhancing (group B) regions of a tumor. Samples are ordered so that the first sample in group A was collected from the same tumor as the first sample in group B and so on. The genes listed above are a sampling from 242 genes that achieved the highest tier of significance (p value = 0.0625). VEGFB is one of many known angiogenic factors while HIF1 α is a gene strongly linked to the development of renal cell carcinoma. Also within this group are several genes involved in glucose metabolism and protein translation that might indicate a higher level of translational activity in enhancing regions vs. non-enhancing regions. Other genes of interest not listed include several cell-cycle activators, cell adhesion molecules, transcription factors, and apoptosis related genes. Differences are displayed as log₂ ratios with negative values indicating increased expression in the enhancing group. Spot images for the genes are displayed below the sample number on the left.

REFERENCES

- 1 Folkman, J. in *Cancer Medicine* (eds Holland, J. F. et al.) 132–152 (Decker, Ontario, Canada, 2000).
- 2 Gullino, PM. Angiogenesis and oncogenesis. *J. Natl Cancer Inst.* 1978;61, 639–643.
- 3 Kaban LB, Mulliken JB, Ezekowitz RA, Ebb D, Smith PS, Folkman J. Antiangiogenic therapy of a recurrent giant cell tumor of the mandible with interferon alfa-2a. *Pediatrics* 1999; 103:1145-1149.
- 4 Ezekowitz RA, Mulliken JB, Folkman J. Interferon alfa-2a therapy for life-threatening hemangiomas of infancy. *N Engl J Med* 1992; 326:1456-1463.
- 5 Weissleder R, Mahmood U. Molecular imaging. *Radiology* 2001 May;219(2):316-33.
- 6 Brasch RC, Li KC, Husband JE, et al. In vivo monitoring of tumor angiogenesis with MR imaging. *Acad Radiol* 2000; 7: 812-823.
- 7 Feng D, Nagy JA, Hipp J, Dvorak HF, Dvorak AM. Vesiculo-vacuolar organelles and the regulation of venule permeability to macromolecules vascular permeability factor, histamine, and serotonin. *J Exp Med* 1996;183:1981–986.
- 8 Qu Hong, Nagy JA, Senger DR, Dvorak HF, Dvorak AM. Ultrastructural localization of vascular permeability factor/vascular endothelial growth factor (VPF/VEGF) to the abluminal plasma membrane and vesiculovacuolar organelles of tumor microvascular endothelium. *J Histochem Cytochem* 1995;43:381–389.
- 9 Stomper PC, Winston JS, Herman S, Klippenstein DL, Arredondo MA, Blumenson LE. Angiogenesis and dynamic MR imaging gadolinium enhancement of malignant and benign breast lesions. *Breast Cancer Res Treat* 1997 Aug;45(1):39-46

- 10 Orel SG, Schnall MD, LiVolsi VA, Troupin RH. Suspicious breast lesions: MR imaging with radiologic-pathologic correlation. *Radiology* 1994 Feb;190(2):485-93
- 11 Stomper PC, Winston JS, Herman S, Klippenstein DL, Arredondo MA, Blumenson LE. Angiogenesis and dynamic MR imaging gadolinium enhancement of malignant and benign breast lesions. *Breast Cancer Res Treat* 1997; 45: 39-46.
- 12 Stomper PC, Winston JS, Herman S, Klippenstein DL, Arredondo MA, Blumenson LE. Angiogenesis and dynamic MR imaging gadolinium enhancement of malignant and benign breast lesions. *Breast Cancer Res Treat* 1997; 45: 39-46.
- 13 Knopp MV, Weiss E, Sinn HP, Mattern J, Junkermann H, Radeleff J, Magener A, Brix G, Delorme S, Zuna I, van Kaick G. Pathophysiologic basis of contrast enhancement in breast tumors. *J Magn Reson Imaging* 1999 Sep;10(3):260-6.
- 14 Hawighorst H, Knapstein PG, Knopp MV, et al. Uterine cervical carcinoma: comparison of standard and pharmacokinetic analysis of time-intensity curves for assessment of tumor angiogenesis and patient survival. *Cancer Res* 1998; 58: 3598-3602.
- 15 Thomas A, Morgan B, Dreves J, et al. Pharmacodynamic results using dynamic contrast enhanced magnetic resonance imaging, of 2 phase 1 studies of the VEGF inhibitor PTK787/ZK 222584 in patients with liver metastases from colorectal cancer. In: *Proceedings of American Society of Clinical Oncology, San Francisco, 2001.* p. A279.
- 16 Knopp MV, Giesel FL, Marcos H, von Tengg-Kobligk H, Choyke P. Dynamic contrast-enhanced magnetic resonance imaging in oncology. *Top Magn Reson Imaging* 2001 Aug;12(4):301-8.

- 17 Knopp MV, Giesel FL, Marcos H, von Tengg-Kobligk H, Choyke P. Dynamic contrast-enhanced magnetic resonance imaging in oncology. *Top Magn Reson Imaging* 2001 Aug;12(4):301-8.
- 18 Brix G, Semmler W, Port R, Schad LR, Layer G, Lorenz WJ. Pharmacokinetic parameters in CNS Gd-DTPA enhanced MR imaging. : *J Comput Assist Tomogr* 1991 Jul-Aug;15(4):621-8
- 19 Knopp MV, Giesel FL, Marcos H, von Tengg-Kobligk H, Choyke P. Dynamic contrast-enhanced magnetic resonance imaging in oncology. *Top Magn Reson Imaging* 2001; 12(4):301-8
- 20 Stomper PC, Herman S, Klippenstein DL, et al. Suspect breast lesions: findings at dynamic gadolinium-enhanced MR imaging correlated with mammographic and pathologic features. *Radiology* 1995; 197: 387-395.
- 21 Mayr NA, Yuh WT, Magnotta VA, et al. Tumor perfusion studies using fast magnetic resonance imaging technique in advanced cervical cancer: a new noninvasive predictive assay. *Int J Radiat Oncol Biol Phys* 1996; 36: 623-633.
- 22 Padhani AR, Hayes C, Assersohn L, Powles T, Leach MO, Husband JE. Response of breast carcinoma to chemotherapy - MR permeability changes using histogram analysis. In: *Proceedings of the 8th Annual Meeting of ISMRM, Denver, 2000.* p 2160.
- 23 Padhani 116,148,149 Padhani AR, O'Donnell A, Hayes C, et al. Dynamic contrast enhanced MR imaging in the evaluation of antiangiogenesis therapy. In: *Molecular Targets and Cancer Therapeutics: Discovery, Development and Cancer Therapeutics:*

- The Joint AACR-NCI-EORTC Meeting, Washington, 1999, Clinical Cancer Research. p 3828S.
- 24 Galbraith SMLM, Taylor NJ, Maxwell R, et al. Combretastatin A4 phosphate reduces tumour blood flow in animal and man, demonstrated by MRI. In: Proceedings of American Society of Clinical Oncology, San Francisco, 2001. p A279.
- 25 Hasan J, Byers R, Jayson GC. Intra-tumoural microvessel density in human solid tumours. *Br J Cancer* 2002; 86(10):1566-77.
- 26 Brix G, Semmler W, Port R, Schad LR, Layer G, Lorenz WJ. Pharmacokinetic parameters in CNS Gd-DTPA enhanced MR imaging. *J Comput Assist Tomogr.* 1991; 15:621 – 727.
- 27 Feldman AL, Costouros NG, Wang E, Qian M, Marincola FM, Alexander HR, Libutti SK. Advantages of mRNA amplification for microarray analysis. *Biotechniques* 2002; 33: 906-12, 914.
- 28 Wang E, Miller LD, Ohnmacht GA, Liu ET, Marincola FM. High-fidelity mRNA amplification for gene profiling *Nat. Biotechnol.* 2000 18, 457-459.
- 29 Mager WH, Planta RJ. Coordinate expression of ribosomalprotein genes in yeast as a function of cellular growth rate. *Mol Cell Biochem.* 1991; 104:181 –187.
- 30 Costouros NG, Lorang D, Zhang Y, Miller MS, Diehn FE, Hewitt SM, Knopp MV, Li, KCP, Choyke PL, Alexander, RH, Libutti SK. Microarray gene expression analysis of murine tumor heterogeneity defined by dynamic contrast enhanced MRI. *Molecular Imaging* 2002; 1 (3): 301-8.
- 31 Davis WK, Boyko OB, Hoffman JM, Hanson MW, Schold SC Jr., Burger PC, Friedman AH, Coleman RE. [18F]-2-fluoro-2-deoxyglucose –positron emission

tomography correlation of gadolinium-enhanced MR imaging of central nervous system neoplasia. *Am J Neuroradiol.* 1993; 14:515 – 523.

32 Brix G, Henze M, Knopp MV, Lucht R, Doll J, Junkermann H, Hawighorst H, Haberkorn U. Comparison of pharmacokinetic MRI and [18F] fluorodeoxyglucose PET in the diagnosis of breast cancer: initial experience. *Eur Radiol* 2001;11(10):2058-70

33 Huang J, Qi R, Quackenbush J, Dauway E, Lazaridis E, Yeatman T. Effects of Ischemia on Gene Expression. *J Surg Res* 99, 222-227 (2001)

**HARVEY CUSHING/JOHN HAY WHITNEY
MEDICAL LIBRARY**

MANUSCRIPT THESES

Unpublished theses submitted for the Master's and Doctor's degrees and deposited in the Medical Library are to be used only with due regard to the rights of the authors. Bibliographical references may be noted, but passages must not be copied without permission of the authors, and without proper credit being given in subsequent written or published work.

This thesis by
has been used by the following person, whose signatures attest their acceptance of the above restrictions.

NAME AND ADDRESS

DATE

YALE MEDICAL LIBRARY



3 9002 01061 5996

